RevMexAA (Serie de Conferencias), **1**, 355-362 (1995)

RESOLVING CIRCUMSTELLAR DISKS WITH THE CSO–JCMT INTERFEROMETER

John E. Carlstrom, Oliver P. Lay
Division of Physics, Mathematics, and Astronomy, MS 105–24
California Institute of Technology Pasadena, CA 91125, USA
Richard E. Hills
MRAO, Cavendish Laboratory, Madingley Road, Cambridge CB3 0HE, U.K.
and
Thomas G. Phillips
Division of Physics, Mathematics, and Astronomy, MS 105–24
California Institute of Technology Pasadena, CA 91125, USA

RESUMEN

Se ha resuelto la emisión compacta de polvo en 870 μm que está asociada a las estrellas jóvenes L1551 IRS 5, HL Tau y a la fuente extremadamente jóven NGC 1333/IRAS 4 usando el nuevo interferómetro CSO–JCMT.

ABSTRACT

The compact dust emission at 870 μm associated with the young stars L1551 IRS 5 and HL Tau and with the extremely young source NGC 1333/IRAS 4 has been resolved using the newly constructed CSO–JCMT interferometer. For HL Tau and L1551, the data are well fit by elliptical Gaussian brightness distributions; these have major axis radii to half-maximum brightness and position angles of 60 AU at 126° for HL Tau, and 80 AU at 162° for L1551. An upper limit of 50 AU (0″.4) is set for the radii along the minor axes, leading to minimum brightness temperatures of 36 K and 28 K, respectively. The elongation is perpendicular to the outflow axes, as expected for accretion disks, and the high brightness indicates substantial column density and mass, further strengthening the accretion disk interpretation. Our observations do not strongly constrain the disk mass; applying an accretion disk model to our data gives lower limits of $\sim$0.02 $M_\odot$. Previous single dish observations of the young protostellar source NGC 1333/IRAS 4 show at least two condensations of dust emission, 4A and 4B, separated by 30″. Our data show considerable structure within each condensation. The visibility data for 4A clearly indicate a binary system with a separation of 1″.8 at position angle 130°; component 4B, although difficult to model with the present data, is also likely to be a binary, making IRAS 4 an embedded quadruple system.

Key words: **ACCRETION, ACCRETION DISKS — STARS: CIRCUMSTELLAR MATTER — STARS: FORMATION — STARS: PRE-MAIN-SEQUENCE**

1. INTRODUCTION

The linking of the CSO (Caltech Submillimeter Observatory) and JCMT (James Clerk Maxwell Telescope) submillimeter telescopes created a powerful instrument for investigating dusty circumstellar disks around nearby young stars. In the Rayleigh–Jeans regime, the thermal continuum flux from dusty circumstellar disks around

low-mass stars is expected to scale as $1/\lambda^2$ or steeper, greatly exceeding the free-free emission at wavelengths shorter than a few mm. The increased optical depth of the dust may also increase the apparent size of the disk. At wavelengths shorter than ~100 μm the residual envelope becomes optically thick, obscuring the central star and disk. Thus imaging of circumstellar disks is best done with high angular resolution observations at submillimeter wavelengths.

The circumstellar disks are expected to be small (~100 AU) and therefore angular resolution of an arcsecond or better is needed to resolve the disks in even the closest star forming regions (D = 140 pc). Interferometry is needed to achieve such high angular resolution; at λ = 870 μm the 164 m baseline of the CSO–JCMT Interferometer provides angular resolution as high as 0″.6, with a typical resolution of ~ 1″.

In this contribution we first briefly describe the observations, with emphasis given to the unique aspects of using a single baseline interferometer. We then discuss the analyses and results of model fitting to the visibility data. Finally we briefly discuss possibilities for future work.

2. OBSERVATIONS

The CSO–JCMT Interferometer comprises the 10.4 m telescope of the Caltech Submillimeter Observatory and the 15 m James Clerk Maxwell Telescope. They are separated by 164 m (189 kλ at λ = 0.87 mm). Technical aspects of the instrument are described by Carlstrom et al. (1993). The single baseline does not allow imaging in the usual sense. Figure 1 shows the u, v coverage and associated beam (point source response) for an earth rotational synthesis at 870 μm. Clearly the imaging capability of the interferometer is limited and the standard deconvolution technique to remove the point source response (CLEAN) is of marginal value. Instead it is much more instructive to fit simple models of the source brightness distribution directly to the measured u, v data.

Observations of HL Tau and L1551 were made on November 12, 1993 over a period of 8 hours. These data have been described previously in Lay et al. (1994). The NGC 1333/IRAS 4 observations were obtained in a similar manner on two separate observing runs. The original data were taken on November 14, 1993 over a period of 10 hours. A continuum bandwidth of 500 MHz was centered on 356.73 GHz. The observations were then repeated with ~50% higher sensitivity on November 1, 1994. Observations of IRAS 4A and IRAS 4B were interleaved with those of the gain calibrator 3C84. The atmosphere limited the coherence time for all observations, so that the visibility phase was used only to vector average the data over 100 s periods. Only the amplitude was used in the subsequent data analyses. As explained in Lay et al. (1994), the measured amplitudes will not be normally distributed and a Rice distribution must be used to determine the goodness of fit to a particular model.

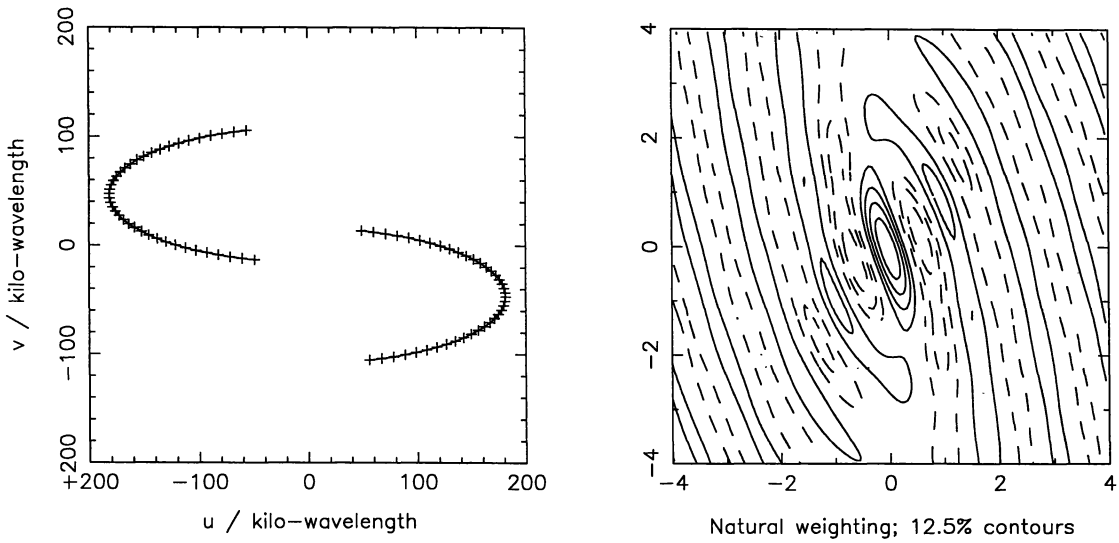

Fig. 1.— The u, v sampling and corresponding beam (point source response pattern) for a source at declination 20 degrees observed for the hour angle range −5 to +5.

3. L1551 IRS 5 AND HL TAU

Figure 2a shows measured flux for HL Tau as a function of projected baseline length. The beam of the interferometer may be envisioned as a corrugated sinusoid pattern on the sky with a period inversely proportional to the projected baseline length. Thus Figure 2a shows that the dust emission toward HL Tau has been resolved. L1551 was also resolved. If the sky brightness is not circularly symmetric then the visibility for a given projected spacing depends on the orientation of the baseline projected against the source. In Figure 2b we show the u, v sampling for HL Tau (L1551 is similar) superimposed on a model of the visibility function for an elliptical Gaussian sky brightness distribution (as shown in the inset). In Figures 2c and 2d we show the measured visibilities as a function of hour angle for HL Tau and L1551, respectively. Note that the minima in the visibilities are not at the same hour angle for each source, indicating different position angles.

The results of the model fitting are summarized in Table 1. Circularly symmetric sky distributions are ruled out. As expected for accretion disks, each source is elongated perpendicular to the axis of a large scale bipolar outflow. The high values for the minimum brightness temperatures indicate substantial optical depths and column densities, further strengthening an accretion disk interpretation.

Our flux for HL Tau accounts for all of the flux detected within a 16″ beam (Adams, Emerson, & Fuller 1990). However, our flux for L1551 is only ~25% of the single dish flux reported by Keene & Masson (1990). Simulations by Lay et al. (1994) show that the flux from a spherical envelope is unlikely to contribute significantly to the flux detected with the interferometer; the interferometer completely 'resolves out' this more extended emission.

We find that even though L1551 is much more embedded and presumably younger than HL Tau, their disks are comparable in size and flux. This suggests that disks are well-established at a relatively early stage in the evolution of a protostar.

Table 1.— Disk parameters

Source	Disk Flux /Jy	γ /deg	r_{maj}[a] /AU	r_{min}[a] /AU	T_b /K	spectral index[b]
L1551	$2.24^{+0.28}_{-0.14}$	162^{+18}_{-9}	80^{+20}_{-10}	< 52	> 28	2.5
HL Tau	$2.52^{+0.42}_{-0.14}$	126^{+18}_{-9}	60^{+10}_{-8}	< 52	> 36	2.7

[a] Radius at half maximum, assuming a distance of 140 pc (Elias 1978). [b] Based on 2.7 mm and 870 μm flux densities. The 2.7 mm data for HL Tau are from: Sargent & Beckwith 1991; Ohashi et al. 1991; Hayashi et al. 1993, and for L1551: Keene & Masson 1990; Ohashi et al. 1991.

4. NGC 1333/IRAS 4A and 4B

IRAS 4 in the region NGC 1333 of the L1450 molecular cloud was originally highlighted as a site of star formation by a pair of highly variable H_2O masers detected by Hashick et al. (1980). Jennings et al. (1987) found a cold, unresolved infrared source at the same position and suggested that pair of masers implied a pair of embedded sources to pump them. This was confirmed by the submillimeter observations of Sandell et al. (1991), which revealed a 30″-separation binary system at a position angle of ~135°, connected by a faint bridge of emission. The components were designated IRAS 4A ($S_{800\ \mu m} \sim 12.7$ Jy, lying to the NW) and IRAS 4B ($S_{800\ \mu m} \sim 8.6$ Jy, lying to the SE). The masses (gas and dust) inferred by Sandell et al. for each component are 9 $M_\odot$ and 4 $M_\odot$ respectively, very high values for sources of this luminosity. They also interpreted the extended nature of IRAS 4A as a large (3200 × 2200 AU) optically thick accretion disk. Observations by Blake et al. (1995) show that IRAS 4A possesses a large, well-collimated outflow; a much more compact outflow is also found for IRAS 4B. They also suggest that masses of 3.5 $M_\odot$ and 1.5 $M_\odot$ are more appropriate. These are still much higher than for normal T Tauri stars, so that both IRAS 4A and 4B are commonly designated

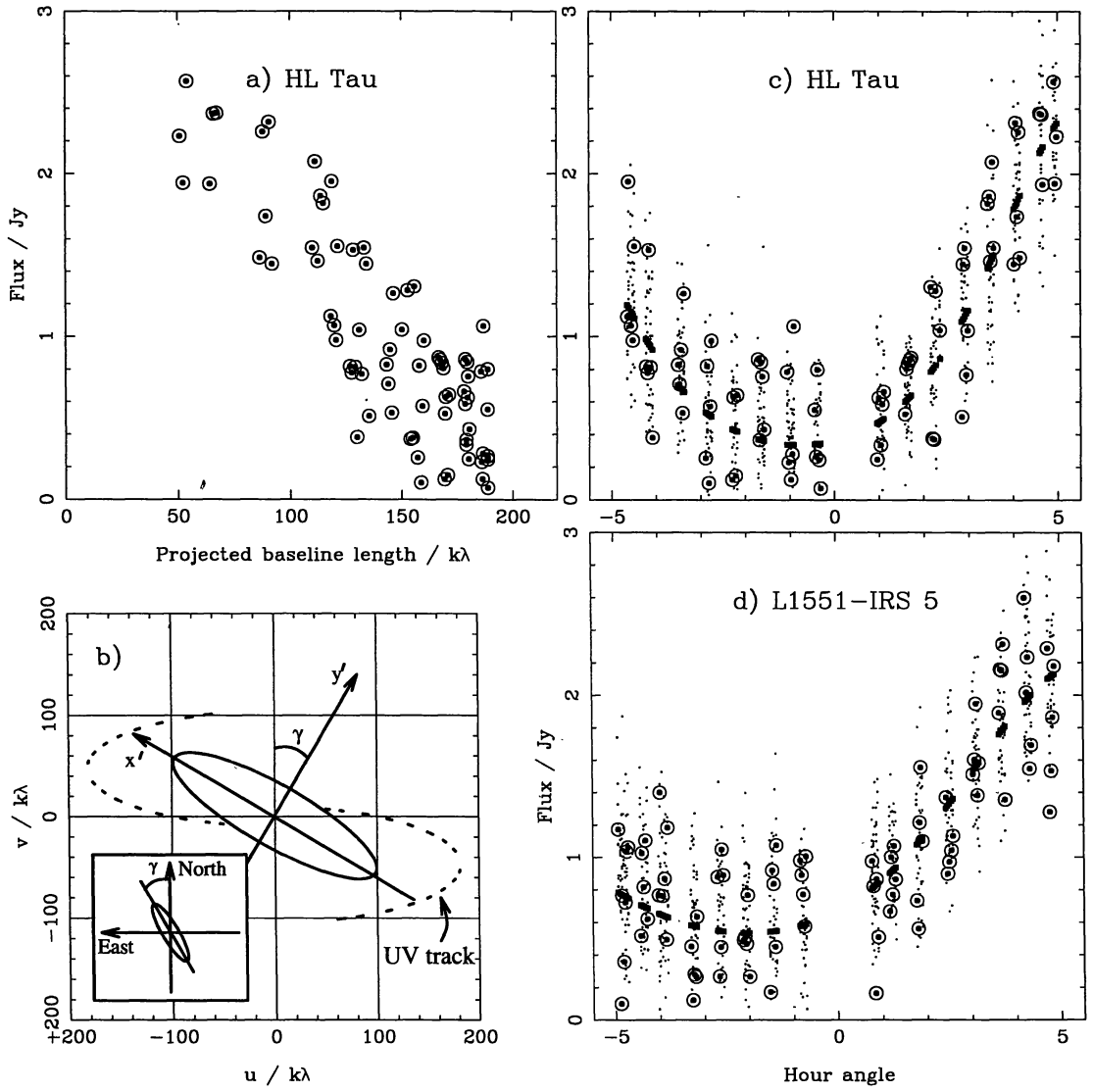

Fig. 2.— (a) The visibility flux of HL Tau at 870 μm detected with the CSO–JCMT Interferometer as a function of the projected baseline length, clearly showing that the emission has been resolved. (b) The Gaussian model used to fit the data, shown in the u, v plane with the track of the interferometer baseline. The inset shows the model as it appears on the sky. (c) & (d) Visibility flux as a function of hour angle for HL Tau and L1551 IRS 5, respectively. The actual data are shown by the circled points and the best-fit model in each case is the series of squares that form a dashed line. The small dots represent the simulated data used to determine the reliability of the fits [Figure taken from Lay et al. (1994)].

'Class 0' protostellar sources in the classification scheme of André, Ward–Thompson, & Barsony (1993) with an estimated age of between 10^4 and 5×10^5 years. The distance to NGC 1333 is usually assumed to be 350 pc (Herbig & Jones 1983) but may be as close as 220 pc (Cernis 1990).

4.1. Results and Analysis

A more complete description of the analysis presented here can be found in Lay et al. (1995). Figure 3 shows the visibility curves for both components, combining the data from both the 1993 and 1994 observations. The fluxes for hour angles beyond ±5 are taken at low elevation where the pointing of the single dishes becomes

inaccurate; these values are therefore expected to be underestimates of the true flux. For hour angles greater then +5 the projected baseline is a minimum and there is likely to be a significant contribution to the visibilities from the more extended, diffuse envelope components. The visibility curves of Figure 3 each show at least two minima. The simple single disk model that was applied to the L1551 and HL Tau data is inadequate in this case, and we must appeal to a binary model to explain the data.

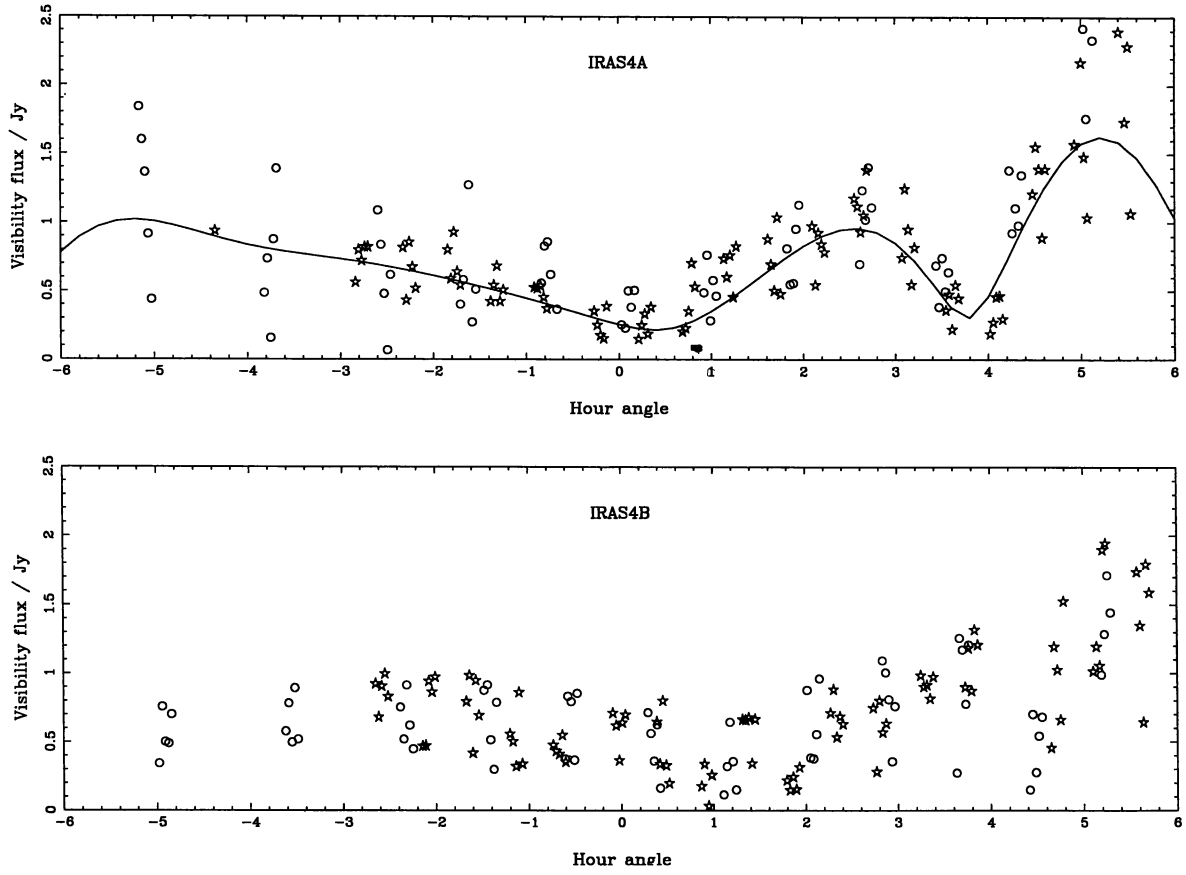

Fig. 3.— Visibility curves for IRAS 4A (top) and IRAS 4B (bottom). Open circles show the November 1993 data; stars show the November 1994 data. The solid line is a binary model fit for IRAS 4A (see below). Note the minima in the visibility flux of IRAS 4B at hour angles of +1.0, +1.9 and +4.2.

The 1-dimensional visibility function for a binary with point source components of equal flux is a cosine curve (the brightness distribution is simply a pair of delta functions). Maxima in the modulus of the visibility occur when the angular separation of the binary is a multiple of the interferometer fringe spacing. In two dimensions the visibility function of a binary with two equal point sources can be pictured as a cosine corrugation in the u, v plane, whose periodicity and orientation are related in a simple manner to the separation and position angle of the binary. As the earth rotates with respect to the source, the interferometer samples a track of positions of the undulating visibility function.

The visibility curve for IRAS 4A is easier to understand than that of IRAS 4B. The two minima in the curve for IRAS 4A, at hour angles of about +1 and +4 constrain the angular separation and the position angle of the binary to values of 1″.8 and 130° respectively. For a binary with one component stronger than the other, the minimum value of the modulus of the visibility function is the difference in flux of the components. In this case, however, the visibility falls to a value close to zero at both minima, indicating that the binary components have similar fluxes at this resolution.

A careful analysis of the visibility curve shows that each component must be extended. It is also possible to constrain the visibility curves for the *individual components*. The surprising result is that one of the components must be elongated at a position angle of ~45° to give a satisfactory fit to the data. This is almost perpendicular to the position angle of the binary, as depicted schematically in Figure 4. This result is independent of the model used to describe the extended emission of each component, but is confirmed by model-fitting that describes each component in terms of elliptical Gaussians (as used for HL Tau and L1551). The fit in Figure 3 is for a binary with separation 1″.8 at 130°. The two components each have a flux of 0.9 Jy; one has a semi-major radius (to half-maximum brightness) of 0″.45 at an angle of 55°, the other a radius of 0″.57 at 145°. This should not be regarded as a unique solution, although the position angle and separation of the binary, equal fluxes of about 1 Jy each and the elongation of one component perpendicular to the binary axis are reliable.

It is harder to find a good fit to the IRAS 4B data, specifically one that reproduces the close minima at hour angles of +1.0 and +1.9. Nevertheless, a binary (or higher multiple system) is almost certainly required. This analysis is currently in progress.

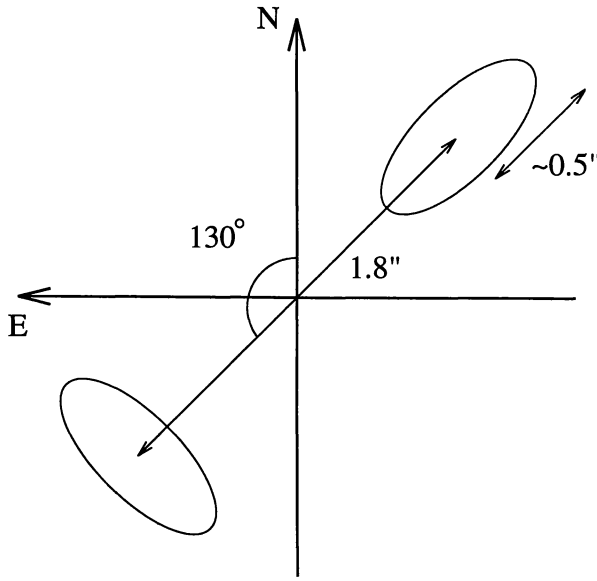

Fig. 4.— Schematic of the model for IRAS 4A. The same model reflected through the origin is equally valid.

4.2. Discussion

The data suggest that both IRAS 4A and 4B are themselves at least binary systems. The interferometer detects only a small fraction of the single dish fluxes seen at 800 μm by Sandell et al. : ~2.0 Jy out of 12.9 Jy for IRAS 4A and ~1.5 Jy out of 8.5 Jy for IRAS 4B. The remaining flux of this young system is probably due to a combination of an extended, possibly infalling envelope and any circumbinary material that might be present but which is resolved out by the interferometer.

Blake et al. (1995) find that the outflow from IRAS 4A appears to be precessing; the large-scale alignment is NE–SW but on smaller scales this becomes more N–S. A binary system provides a natural explanation for this precession. By estimating the rate of precession from the outflow, it may be possible to constrain the masses of the two components. Precession might also explain why one of the components appears to be elongated approximately *parallel* to the outflow direction of the IRAS 4A system.

The sizes and fluxes implied for the binary components of IRAS 4A are consistent with dusty accretion disks. An estimated angular radius of 0″.5 corresponds to ~170 AU for a distance of 350 pc, or ~110 AU if the

Table 2.— Apparent disk size as a function of wavelength[a]

Telescope	λ_{obs}	$r_{\tau_1}(\beta = 1)$	$r_{\tau_1}(\beta = 2)$
CSO-JCMT	350μm	**1".20**	**3".1**
CSO-JCMT	600μm	**0".73**	**1".1**
CSO-JCMT	870μm	**0".50**	**0".50**
CSO-JCMT	1.3mm	0".33	0".22
BIMA, IRAM, NRO, OVRO	1.3mm	0".33	0".22
BIMA, IRAM, NRO, OVRO	3.0mm	0".15	0".04
VLA	7.0mm	**0".06**	0".008
VLA	7.0mm	0".03	0".002

[a]Angular sizes in bold face type can be resolved by the instrument listed.

distance is 220 pc. If the disk of L1551 IRS 5 (2.2 Jy at a distance of 140 pc) were to be placed at a distance of 220 pc it would have a flux of 0.9 Jy and an angular size of about 90 AU, very similar to the values we infer for the IRAS 4A components.

5. FURTHER REMARKS

The CSO–JCMT submillimeter-wave interferometer is well-suited to probing the innermost regions of cool circumstellar material associated with young stars. Several observations in addition to those described above are being pursued: searching for infalling gas by looking for redshifted absorption lines against the bright dust continuum emission; determining the nature of the dust continuum emission toward Ae/Be stars (disk, envelope or additional sources?); searching for other binary systems and probing the individual and circumbinary disks; determining detailed velocity structure of circumstellar masers, as has been done at longer wavelengths (see Plambeck, Wright, & Carlstrom 1990; Planesas, Martín–Pintado, & Serabyn 1992).

The interferometer will eventually be capable of observing at wavelengths as short as 300 μm. The first test at 600 μm was made in November 1994. Measuring accretion disks at several different frequencies will allow us to test protostellar accretion disk theories. In the standard model the disk surface density scales roughly as $\Sigma(r) \propto 1/r$, so the optical depth through the disk scales as $\tau_\lambda = \kappa_\beta \Sigma \propto (1/\lambda)^\beta (1/r)$. The dust emissivity κ is fairly uncertain in magnitude, but should scale as $(1/\lambda)^\beta$, with β between 1 and 2 for a reasonable composition of dust grains. Therefore the radius at which $\tau = 1$ for an accretion disk should scale as $(1/\lambda)^\beta$. Table 2 lists r_{τ_1} as a function of wavelength for $\beta = 1$ and for $\beta = 2$. The radii given in Table 2 are normalized to 0".5 at 870 μm, approximately the radius that we determined for the HL Tau and L1551 disks. We do not know that our measured radii reflect r_{τ_1}, but it is clear from the large variation in size shown in Table 2 that multi-wavelength measurements will allow better constraints to be placed on the dust opacity law and models of accretion disks.

REFERENCES

Adams, F. C., Emerson, J. P., & Fuller, G. A. 1990, ApJ, 357, 606
André, P., Ward-Thompson, D., & Barsony, M. 1993, ApJ, 406, 122
Blake, G. A., Sandell, G., van Dishoeck, E. F., Groesbeck, T. D., Mundy. L. G., & Aspin, C. 1995, ApJ, in press
Carlstrom, J. E., Hills, R. E., Lay, O. P., Force, B. F., Hall, C. G., Phillips, T. G. & Schinckel, A. E. 1993, in Astronomy with Millimeter and Submillimeter Wave Interferometry (IAU Colloquium 140), ed. M. Ishiguro & W. J. Welch, ASP Conf. Ser., 59, 35
Cernis, K. 1990, A&SS, 166, 315
Elias, J. 1978, ApJ, 224, 857

Haschick, A. D., Moran, J. M., Rodríguez, L. F., Burke, B. F., Greenfield, P., & García–Barreto, J. A. 1986, ApJ, 237, 26
Hayashi, M., Ohashi, N., & Miyama, S. 1993, ApJ, 418, L71
Herbig, G. H., & Jones, B. F. 1983, AJ, 88, 1040
Jennings, R. E., Cameron, D. M. H., Cudlip, W., & Hirst, C. J. 1987, MNRAS, 226, 461
Keene, J., & Masson, C. R. 1990, ApJ, 355, 635
Lay, O. P., Carlstrom, J. E., Hills, R. E., & Phillips, T. G. 1994, ApJ, 434, L75
Lay, O. P., Carlstrom, J. E., Hills, R. E., & Phillips, T. G. 1995, in preparation
Ohashi, N., Kawabe, R., Hayashi, M., & Ishiguro, M. 1991, AJ, 102, 2054
Plambeck, R. L., Wright, M. C. H., & Carlstrom, J. E. 1990, ApJ, 348, L65
Planesas, P., Martín–Pintado, J., & Serabyn, E. 1992, ApJ, 386, L23
Sandell, G., Aspin, C., Duncan, W. D., Russell, A. P. G., & Robson, E. I. 1991, ApJ, 376, L17
Sargent, A. I, & Beckwith, S. V. W. 1991, ApJ, 382, L31